



## Short communication

## Effect of nanosized silica in poly(methyl methacrylate)–lithium bis(trifluoromethanesulfonyl)imide based polymer electrolytes

S. Ramesh\*, Soon-Chien Lu

Faculty of Engineering &amp; Science, Universiti Tunku Abdul Rahman, Setapak, 53300 Kuala Lumpur, Malaysia

## ARTICLE INFO

## Article history:

Received 29 May 2008

Received in revised form 30 June 2008

Accepted 9 July 2008

Available online 30 July 2008

## Keywords:

Polymer electrolytes

Poly(methyl methacrylate)

Lithium bis(trifluoromethanesulfonyl)imide

Silica

Conductivity

Solid-state battery

## ABSTRACT

The effect of nanosized silica when incorporated in polymer electrolytes is analyzed by means of Fourier transform infrared (FTIR) spectroscopy, conductivity and thermal properties. Nanocomposite polymer electrolytes are synthesized by the dispersion of nanosized silica ( $\text{SiO}_2$ ), up to 10 wt.% maximum, into a matrix formed by poly(methyl methacrylate) (PMMA) and lithium bis(trifluoromethanesulfonyl)imide (LiTFSI). The highest conductivity is  $2.44 \times 10^{-6} \text{ S cm}^{-1}$  at room temperature, with 4 wt.% of silica added. The FTIR spectra show evidence of complexation between PMMA, LiTFSI and  $\text{SiO}_2$ . The addition of silica to the polymer electrolytes also improves the thermal stability and the ability to retain conductivity over time.

© 2008 Elsevier B.V. All rights reserved.

## 1. Introduction

Composite polymer electrolytes (CPEs) are widely studied because of their potential application in a variety of electrochemical devices, such as solid-state batteries, electrochromic windows, sensors, and fuel cells [1]. They are attractive candidates for next-generation lithium batteries as they are capable of overcoming the limitations of conventional liquid electrolytes such as lithium dendrite formation, electrolyte leakage, flammable organic solvent, and electrolytic degradation of electrolytes [2–5]. Initial studies were focused on gel polymer electrolytes (GPEs) based on poly(methyl methacrylate) (PMMA) and polyacrylonitrile (PAN). The PMMA-based GPEs preferred due to their lightweight, high light transmittance, chemical resistance, colourless nature, resistance to weathering corrosion, and good insulating properties [6].

In addition to possessing the many desirable properties mentioned above, PMMA also has an amorphous morphology and a polar functional group in its polymer chain that exhibits a high affinity for lithium ions and plasticizing solvents. Due to these characteristics, Iijima et al. [7] were the first researchers to employ PMMA as a polymer host material in the development of a polymer-based electrolyte. The addition of liquid plasticizers, organic acids

and inert fillers has also been used to improve the conductivity of polymer electrolytes [2,8,9]. The most serious limitation of the plasticized gel-based PMMA system is its poor mechanical property [10]. Adding liquid plasticizers to the polymer matrix may effectively increase the conductivity by forming a GPE. On the other hand, the mechanical properties and stability with lithium metal ions are poor in the presence of a large fraction of liquid [2].

One way to improve the mechanical strength of these composites is to incorporate inorganic/ceramic fillers [11,12], which may also enhance the ionic conductivity [13]. In particular, the automotive industry requires low-cost, lightweight and high-performance materials, suitable for processing on existing machinery. Nanocomposite polymer electrolytes can meet many of these requirements [14]. It is well accepted that the fillers play an important role in lithium-ion transport, but different trends in conductivity due to the addition of fillers have been observed. For instance, an increase, a decline or no change in conductivity have all been reported before, but the observed effect is much less than that found with the addition of an extra polymer in GPEs. This apparent discrepancy can be attributed partially to the difference in electrolyte materials (polymers, salt and filler type), as well as to the concentration and preparation of the starting materials [1].

Composite electrolytes containing a polymer host, doping salt and ceramic filler were first synthesized by Weston and Steele [11]. Common fillers include silica ( $\text{SiO}_2$ ), magnesia (MgO),  $\text{LaMnO}_3$ , alumina ( $\text{Al}_2\text{O}_3$ ), titania ( $\text{TiO}_2$ ), and ceria ( $\text{CeO}_2$ ) [9,15–19]. Fumed silica

\* Corresponding author. Tel.: +60 3 4107 9802; fax: +60 3 4107 9803.  
E-mail address: [ramesh@mail.utar.edu.my](mailto:ramesh@mail.utar.edu.my) (S. Ramesh).

**Table 1**  
Designations of (PMMA–LiTFSI):SiO<sub>2</sub> polymer electrolyte thin films

Compositions of PMMA–LiTFSI:SiO <sub>2</sub> (wt.%)	Designation
100:0	CPE-0
98:2	CPE-2
96:4	CPE-4
94:6	CPE-6
92:8	CPE-8
90:10	CPE-10

is of special interest because of its branched primary structure and the ability to tailor the surface functionalities. The effect induced by fillers is ascribed to an increase in the volume fraction of the amorphous phase, which is a prerequisite for higher conductivity. Composite polymer electrolytes based on fumed silica were shown to be highly transparent in the visible region and to have a wide electrochemically stable potential window [20].

Other than the methods of maximizing the conductivity of polymer electrolyte mentioned above, the polymer electrolyte properties may also be influenced by the lithium salt. This is due to the fact that the anion has an important influence on both the phase composition and the conductivity [21]. More success has been achieved with non-coordinate anions with extensive charge delocalization. The significant breakthrough has been with bis(trifluoromethanesulfonyl)imide lithium salt, abbreviated as LiTFSI and used in this work. Such molecules are mechanically flexible and have both a large electronegativity and a large delocalization of charge.

## 2. Experimental

### 2.1. Materials

Poly(methyl methacrylate) with an average  $M_w = 35,000$  was obtained from Acros Organic. Lithium bis(trifluoromethanesulfonyl)imide salt, LiTFSI [LiN(CF<sub>3</sub>SO<sub>2</sub>)<sub>2</sub>], was obtained from Fluka and dried at 100 °C for 1 h to eliminate trace amounts of water in the material, prior to the preparation of composite polymer electrolytes. Fumed silica (SiO<sub>2</sub>) with 7 nm particle size and tetrahydrofuran (THF) were obtained from J.T. Baker and Aldrich, respectively.

### 2.2. Preparation of thin films

Several nanocomposite polymer electrolyte complexes were prepared; the compositions are listed in Table 1. The thin films were prepared by the solution casting technique with THF as solvent. The mixture was cast in a Petri dish and allowed to evaporate slowly inside a fume hood. This procedure yields mechanically stable and free-standing films. The thickness of the films was measured by means of a micrometer screw gauge.

### 2.3. Instrumentation

#### 2.3.1. Fourier transform infrared (FTIR) analysis

The FTIR studies were performed with a Perkin-Elmer FTIR Spectrometer, Spectrum RX1, in the wave region between 4000 and 400 cm<sup>-1</sup>, with a resolution of 4 cm<sup>-1</sup>.

#### 2.3.2. Impedance spectroscopy

The samples were cut and sandwiched between two stainless-steel blocking electrodes. A HIOKI 3532-50 LCR Hi-Tester was used to perform the impedance measurements for each electrolyte film over the frequency range of 50 Hz to 1 MHz.

#### 2.3.3. Thermal analysis

Thermogravimetric analysis (TGA) was undertaken with a Mettler Toledo analyzer that consisted of a TGA/SDTA851<sup>e</sup> main unit and STARE software with a 10 °C min<sup>-1</sup> heating rate between 30 and 400 °C in nitrogen.

## 3. Results and discussion

### 3.1. FTIR studies

FTIR spectroscopy is a valuable technique for investigating interactions in polymer electrolytes. The FTIR spectra of such electrolytes vary as a result of different compositions and the occurrence of complexation and interaction between the various constituents [22], which may shift the polymer cage peak. FTIR is used to determine the occurrence of complexation in a crystalline or an amorphous phase [23].

FTIR spectra are recorded in the transmittance mode. The FTIR spectra of pure PMMA, pure LiTFSI, CPE-0, pure nanosized fumed silica and CPE-2 are presented shown in Fig. 1. Some band assignments for PMMA and silica have already been reported and are listed in Table 2 [15,24,25].

The bands mentioned in Table 2 are also observed in Fig. 1(a) and (b). For PMMA, CH<sub>2</sub> rocking is observed at 750 cm<sup>-1</sup>, –O–CH<sub>3</sub> at 1388 cm<sup>-1</sup>, –CH<sub>3</sub> at 1458 cm<sup>-1</sup>, H–CO–O–C at 1734 cm<sup>-1</sup>, C–O–CH<sub>3</sub> at 2954 cm<sup>-1</sup>, and asymmetric CH<sub>2</sub> stretching at 2992 cm<sup>-1</sup>. On the other hand, for LiTFSI, S–N stretching is found at 740 cm<sup>-1</sup>, a combination of C–S and S–N stretching at 787 cm<sup>-1</sup>, S=O bonding at 1065 cm<sup>-1</sup>, C–SO<sub>2</sub>–N bonding at 1142, 1333 and 1356 cm<sup>-1</sup>, –CF<sub>3</sub> at 1193 cm<sup>-1</sup>, and S–CH<sub>3</sub> at 2876 and 2979 cm<sup>-1</sup>.

The FTIR spectrum of sample CPE-0 in Fig. 1(c), which contains PMMA:LiTFSI (70:30), contains a new intense peak at 917 cm<sup>-1</sup>. The peak of –CF<sub>3</sub> in LiTFSI at 1193 cm<sup>-1</sup> is shifted to 1188 cm<sup>-1</sup>. The peak of –CH<sub>3</sub> in PMMA at 1458 cm<sup>-1</sup> shifts to 1459 cm<sup>-1</sup> and is more intense. The peak of H–CO–O–C in PMMA at 1734 cm<sup>-1</sup> has become sharper and more intense. The peaks of S–CH<sub>3</sub> in LiTFSI at 2876 cm<sup>-1</sup> and asymmetric CH<sub>2</sub> stretching in PMMA at 2992 cm<sup>-1</sup> have become more intense and have shifted to 2830 and 2991 cm<sup>-1</sup>, respectively. There is also overlapping of the two peaks of C–O–CH<sub>3</sub> in PMMA at 2954 cm<sup>-1</sup> and S–CH<sub>3</sub> in LiTFSI at 2979 cm<sup>-1</sup> and the formation of an intense peak at 2909 cm<sup>-1</sup>.

In the FTIR spectrum of nanosized silica shown in Fig. 1(d), the characteristic peaks of silica are observed at 809, 1103, 1636 and 3423 cm<sup>-1</sup> [15]. In the FTIR spectrum of CPE-2 in Fig. 1(e), after the addition of silica, many of the peaks that are present in CPE-0 and silica disappear or become less intense, including those at 917, 1103, 1459, 2830, 2909 and 2991 cm<sup>-1</sup>. The formation of a new peak at 991 cm<sup>-1</sup> is also observed in CPE-2, as reported by Subban and Arof [15].

The disappearance and shifting of some bands, the formation of new peaks and changes in the intensity of the peaks in the FTIR spectra of nanocomposite polymer electrolytes suggest that some degree of co-ordination or complexation has occurred between the PMMA, LiTFSI and nanosized silica. In summary, these observations establish the complexation of LiTFSI and SiO<sub>2</sub> with PMMA.

### 3.2. Alternating current (AC) impedance studies

The variation of log conductivity values as a function of nanosized silica concentration is shown in Fig. 2. As can be seen, the conductivity decreases when 2 wt.% of silica is first added to the PMMA/LiTFSI system, followed by a significant increase at 4 wt.% of silica addition. After that, the conductivity decreases again and remains relatively constant upon addition of silica up to 10 wt.%.

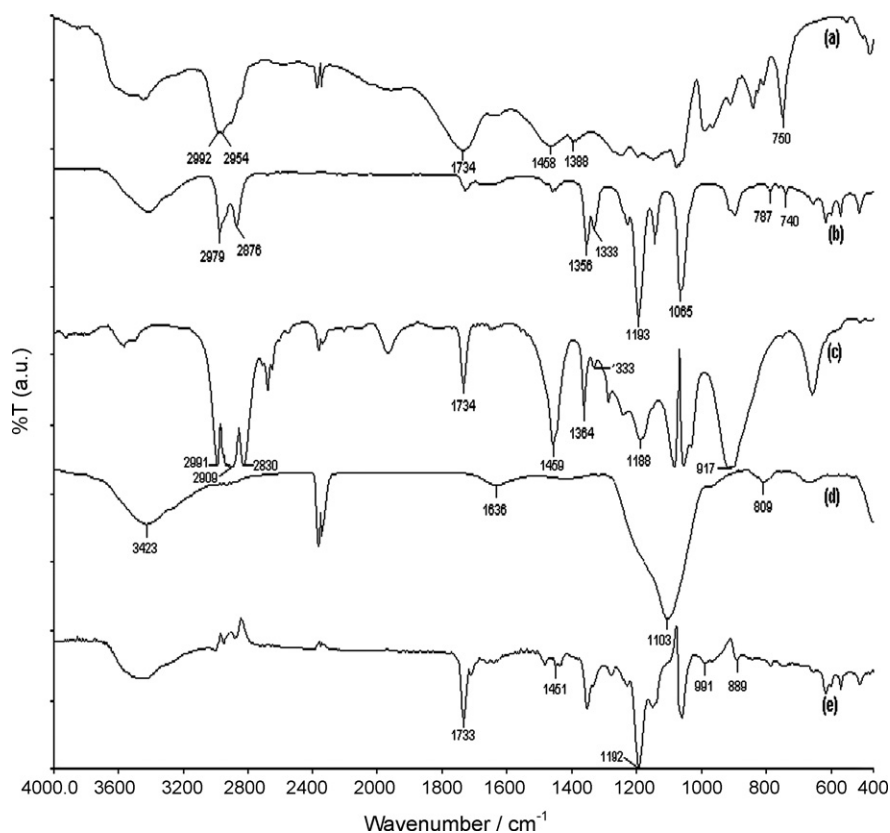


Fig. 1. FTIR spectra of (a) pure PMMA, (b) pure LiTFSI, (c) CPE-0, (d) pure nanosized fumed silica and (e) CPE-2.

The above findings are in agreement with those described in the literature, where it has been observed that a maximum in the conductivity occurs as the inorganic filler concentration is increased, followed by a decrease in conductivity values for higher filler concentration [15,16,24]. When silica is first added to the PMMA/LiTFSI system, the conductivity decreases due to blocking of existing conducting pathways and the possible conglomeration of the excess silica, which reduces the polymer–filler interface and hence reduces the conducting pathways. As the silica content is increased to 4 wt.%, conducting pathways are again created but for the conduction of TFSI anions. Further increase in filler content results in the blocking and the termination of the formation of conducting pathways [15]. The conductivity of the highest conducting sample, CPE-4, is calculated to be  $2.44 \times 10^{-6} \text{ S cm}^{-1}$  at room tem-

perature. The Cole–Cole impedance plot of sample CPE-4 is shown in Fig. 3. To calculate the conductivity of a thin film sample, the following relationship can be used:

$$\sigma = \frac{l}{R_b A} \quad (1)$$

where  $\sigma$  is the conductivity in  $\text{S cm}^{-1}$ ,  $l$  is the thickness of thin film sample in cm,  $R_b$  is the bulk resistance in  $\Omega$  obtained from Cole–Cole impedance plot as in Fig. 3 and  $A$  is the surface area of the stainless-steel blocking electrodes in  $\text{cm}^2$ .

The interfacial properties of composite polymer electrolytes play an important role in practical applications. In order to eval-

Table 2

Some important peaks in FTIR spectra of pure PMMA, pure LiTFSI, CPE-0, pure nanosized fumed silica and CPE-2, and their assignments

Wavenumber ( $\text{cm}^{-1}$ )	Group/species with their possible assignments
740	S–N stretching in LiTFSI
750	$\text{CH}_2$ rocking in PMMA
787	Combination of C–S and S–N stretching in LiTFSI
809, 1636	Characteristic peaks of silica
1065	S=O in LiTFSI
1103	Si–O–Si in silica
1142, 1333, 1356	C– $\text{SO}_2$ –N in LiTFSI
1193	– $\text{CF}_3$ in LiTFSI
1388	–O– $\text{CH}_3$ in PMMA
1458	– $\text{CH}_3$ in PMMA
1734	H–CO–O–C in PMMA
2876, 2979	S– $\text{CH}_3$ in LiTFSI
2954	C–O– $\text{CH}_3$ in PMMA
2992	Asymmetric $\text{CH}_2$ stretching in PMMA
3423	Si–OH of surface hydroxyl group in fumed silica

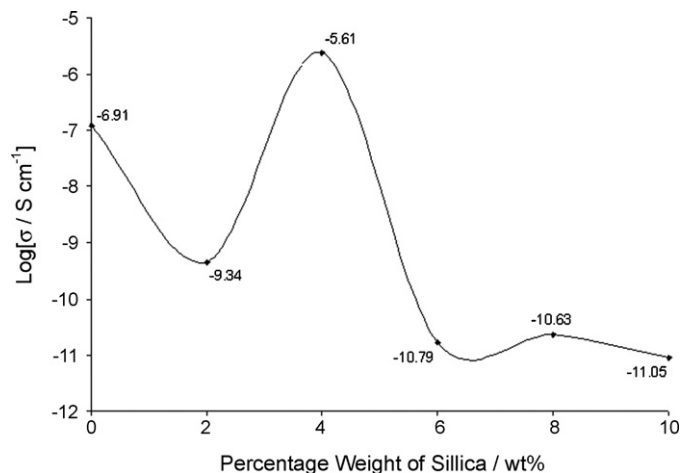


Fig. 2. Variation of log conductivity as function of weight percentage of nanosized silica added in (PMMA–LiTFSI): $\text{SiO}_2$  complexes.

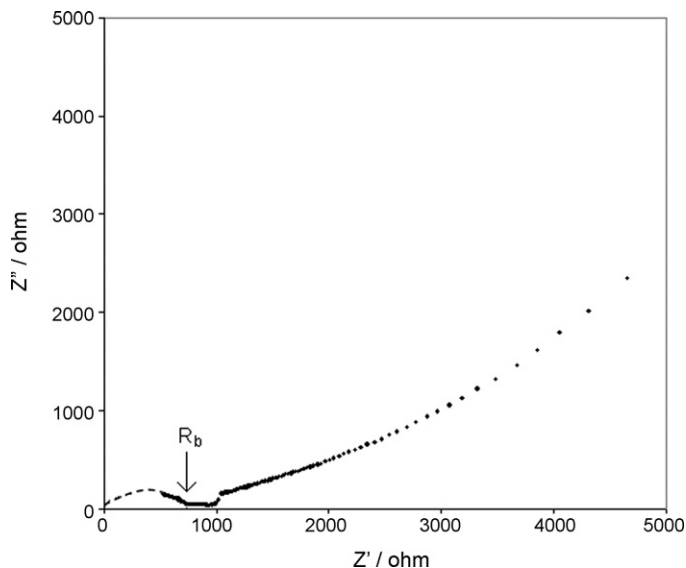


Fig. 3. Cole–Cole impedance plot for highest conducting sample: CPE-4.

uate the ionic conductivity of the samples over time, samples with (CPE-2) and without nanosized silica (CPE-0) are chosen. Their conductivities are measured for 30 days and the results are given in Fig. 4. It is seen that the decrease in conductivity of CPE-2 is relatively lower than that of CPE-0. This means that the addition of nanosized silica has improved the ability to retain the conductivity of CPEs. This effect has been explained by Stephan et al. [26] that the addition of the nanosized fillers traps any remaining traces of organic solvent impurities. This may account for the enhanced interfacial stability of the nanocomposite polymer electrolytes and it can also be concluded that the passivation process may basically involve a reaction between the lithium metal and the anions of the lithium salt with the formation of a thin, compact inorganic-layer and favours good lithium cycleability. After 10 days, the conductivities of both samples become relatively unchanged. It can be assumed that the morphology of the passivation films change with time to acquire finally a non-compact, possibly porous, structure.

### 3.3. Thermal studies

The weight loss of pure PMMA, CPE-0 and CPE-4 was evaluated by TGA in nitrogen gas. The results are presented in Fig. 5. The

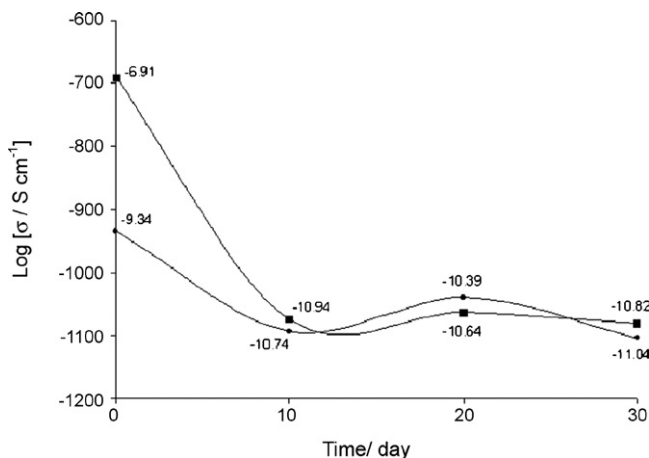


Fig. 4. Variation of log conductivity at room temperature with time for samples with (● as CPE-2) and without nanosized silica (■ as CPE-0).

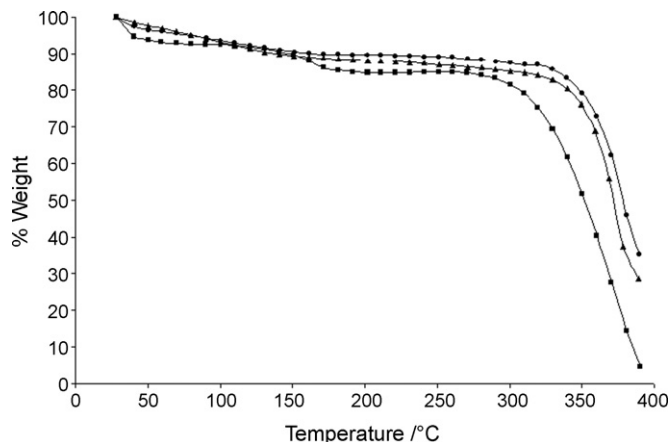


Fig. 5. Normalization of dynamic TGA in nitrogen gas for pure PMMA (■), CPE-0 (▲) and CPE-4 (●).

Table 3

Decomposition temperatures and percentages of total weight loss of pure PMMA, CPE-0 and CPE-4 in TGA

Sample	Decomposition temperature (°C)	Total weight loss (%)
Pure PMMA	359.37	95.17
CPE-0	369.29	71.46
CPE-4	372.46	64.83

decomposition temperatures and percentages of total weight loss of the same samples obtained from TGA are listed in Table 3. Particle addition leads to a temperature shift of the onset of weight loss. According to García et al. [27], the addition of small amounts of silica particles eliminates the formation of the first radical in the depolymerisation process through chain ends of both depolymerisation and side group elimination, in the absence of oxygen. The decomposition temperature also increases upon addition of LiTFSI and nanosized silica, which indicates that the nanocomposite polymer electrolyte formed is more heat resistant. From Fig. 5, it can also be seen that the addition of nanosized silica has significantly enhanced the thermal stability of the polymer electrolytes.

## 4. Conclusions

Nanocomposite polymer electrolytes have been synthesized by dispersing up to 10 wt.% of nanosized silica in the matrix formed by PMMA and LiTFSI. The addition of nanosized silica affects the FTIR spectra, ionic conductivity and thermal properties of polymer electrolytes based on the PMMA/LiTFSI system. The highest conductivity obtained is  $2.44 \times 10^{-6} \text{ S cm}^{-1}$  at room temperature, with 4 wt.% of silica added. The FTIR spectra show some complexation between PMMA, LiTFSI and  $\text{SiO}_2$ . The addition of silica also improves the thermal stability and the ability to retain conductivity over time of the polymer electrolytes.

## References

- [1] S. Ahmad, S. Ahmad, S.A. Agnihotry, J. Power Sources 140 (2005) 151–156.
- [2] Y. Li, J.A. Yerian, S.A. Khan, P.S. Fedkiw, J. Power Sources 161 (2006) 1288–1296.
- [3] P.G. Bruce, C.A. Vincent, J. Chem. Soc., Faraday Trans. 89 (1993) 3187.
- [4] M. Armand, Solid State Ionics 69 (1994) 309–319.
- [5] H.J. Gores, J.M.G. Barthel, Pure Appl. Chem. 67 (1999) 919.
- [6] F. Latif, M. Aziz, N. Katun, A.M.M. Ali, M.Z. Yahya, J. Power Sources 159 (2006) 1401.
- [7] T. Iijima, Y. Toyoguchi, N. Eda, Denki Kagaku 53 (1985) 619.
- [8] J.W. Park, E.D. Jeong, M. Won, Y. Shima, J. Power Sources 160 (2006) 674–680.
- [9] H.M.J.C. Pitawala, M.A.K.L. Dissanayake, V.A. Seneviratne, Solid State Ionics 178 (2007) 885–888.
- [10] K. Yuichi, K. Kishino, N. Koichi, J. Appl. Polym. Sci. 63 (3) (1997) 363.

- [11] J.E. Weston, B.C. Steele, *Solid State Ionics* 7 (1982) 75–79.
- [12] J. Cho, M. Liu, *Electrochim. Acta* 42 (1997) 1481–1488.
- [13] E. Quartarone, P. Mustarelli, A. Magistris, *Solid State Ionics* 110 (1989) 1–14.
- [14] M. Katsikis, F. Zahradnik, A. Helmschrott, H. Münstedt, A. Vital, *Polym. Degrad. Stab.* 92 (2007) 1966–1976.
- [15] R.H.Y. Subban, A.K. Arof, J. New Mater. *Electrochem. Syst.* 6 (2003) 197–203.
- [16] R. Kumar, A. Subramania, N.T.K. Sundaram, G.V. Kumarb, I. Baskaran, *J. Membr. Sci.* 300 (2007) 104–110.
- [17] T. Kuila, H. Acharya, S.K. Srivastava, B.K. Samantaray, S. Kureti, *Mater. Sci. Eng. B* 137 (2007) 217–224.
- [18] M. Moskwia, I. Giska, R. Borkowska, A. Zalewska, M. Marczewski, H. Marczewska, W. Wieczorek, *J. Power Sources* 159 (2006) 443–448.
- [19] A. Dey, S. Karan, S.K. De, *Solid State Ionics* 178 (2008) 1963–1968.
- [20] S.A. Agnihotry, S. Ahmad, D. Gupta, S. Ahmad, *Electrochim. Acta* 49 (2004) 2343–2349.
- [21] S. Ramesh, F.Y. Tai, J.S. Chia, *Spectrochim. Acta Part A: Mol. Biomol. Spectrosc.* 69 (2007) 670–675.
- [22] S. Ramesh, K.H. Leen, K. Kumutha, A.K. Arof, *Spectrochim. Acta Part A* 66 (2007) 1237–1242.
- [23] S. Rajendran, T. Uma, *Mater. Lett.* 44 (2000) 208–214.
- [24] J.P. Sharma, S.S. Sekhon, *Solid State Ionics* 178 (2007) 439–445.
- [25] S. Ahmad, M. Deepa, S.A. Agnihotry, *Sol. Energy Mater. Sol. Cells* 92 (2008) 184–189.
- [26] A.M. Stephan, K.S. Nahm, M.A. Kulandainathan, G. Ravi, J. Wilson, *Eur. Polym. J.* 42 (2006) 1728–1734.
- [27] N. García, T. Corrales, J. Guzmán, P. Tiemblo, *Polym. Degrad. Stab.* 92 (2007) 635–643.